LBL-15701
c.2

Lawrence Berkeley Laboratory
UNIVERSITY OF CALIFORNIA

EARTH SCIENCES DIVISION

Presented at the Third National Symposium on Aquifer Restoration and Groundwater Monitoring, Columbus, OH, May 25-27, 1983

A STUDY OF CONTAMINANT PLUME CONTROL IN FRACTURED-POROUS MEDIA

C.F. Tsang, D.C. Mangold, C. Doughty, and I. Javandel

May 1983

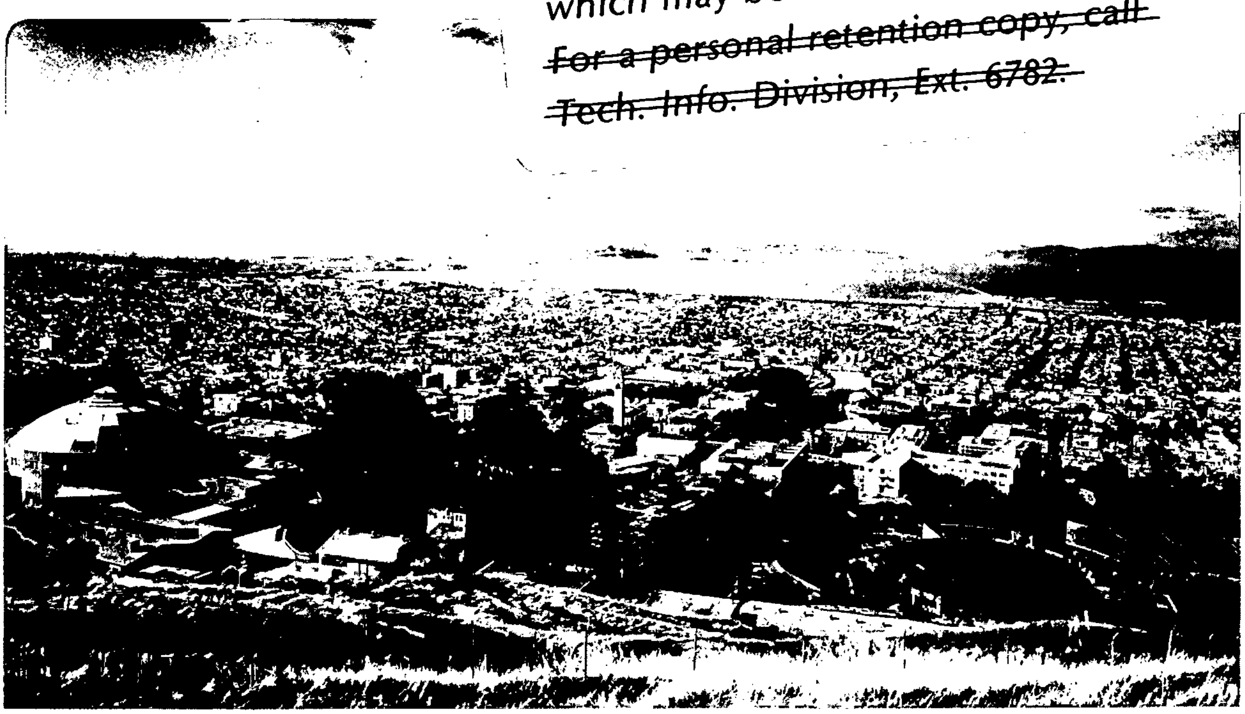

Prepared for the U.S. Department of Energy under Contract DE-AC03-76SF00098

DISCLAIMER

A STUDY OF CONTAMINANT PLUME CONTROL IN FRACTURED-POROUS MEDIA

Chin Fu Tsang, Donald C. Mangold, Christine Doughty, and Iraj Javandel

Earth Sciences Division
University of California
Lawrence Berkeley Laboratory
Berkeley, California 94720

Abstract

Mathematical modeling studies have been made on the control, containment, and removal of contaminant plumes in water-saturated, fractured, porous media. Two approaches have been investigated from a hydrological point of view. The first considers one or more low-permeability barriers to contain the plume and to prevent it from being carried away by natural, regional groundwater flow. The second studies various plume extraction schemes using a pumping well. Heterogeneous and fractured aquifers are considered as well as a contaminant plume that is heavier than the groundwater. General discussions on the effectiveness and limits of the various plume control procedures are discussed.

A STUDY OF CONTAMINANT PLUME CONTROL IN FRACTURED-POROUS MEDIA

Chin Fu Tsang, Donald C. Mangold, Christine Doughty, and Iraj Javandel

Earth Sciences Division
University of California
Lawrence Berkeley Laboratory
Berkeley, California 94720

Introduction

When a contaminant plume is encountered in an aquifer, several measures may be taken to control, contain or remove the plume. In the present study two such measures are investigated from a hydrological point of view. The first involves installation of a low permeability barrier to contain the plume and prevent it from being carried away by natural, regional groundwater flow. Questions often arise concerning the optimal length of the barrier, and the possible need for more than one barrier for the containment of the plume. The second measure is extraction of the contaminant plume by means of a pumping well. In this case one must decide on the optimal pumping depth.

This paper presents the results of numerical simulation studies for a series of scenarios involving the use of barriers or a pumping well to contain or remove a contaminant plume from an aquifer. Important features of plume control that are considered here include aquifer heterogeneity due to permeability layering or a fracture zone, and a contaminant plume that is denser than the groundwater.

Methodology

The calculational results presented in this paper are based on the numerical code CPT [1]. The code involves a number of partial differential equations that describe the three-dimensional flow of fluids in a complex porous medium with or without the presence of discrete fractures. The code CPT, which was developed at the Lawrence Berkeley Laboratory, employs the Integrated-Finite-Difference (IFD) numerical scheme and calculates coupled thermohydrologic flows with simple chemical advective transport and reactions. The formulation includes the effects of density and viscosity variations of the fluid, gravitation or buoyancy effects, aquifer heterogeneity and complex boundary conditions. Molecular diffusion and hydrodynamic dispersion are not considered. The code CPT has been derived from an earlier version called PT [2], which has been verified against eight analytical or semi-analytical solutions and validated against a series of four field experiments [3,4].

Comparative Studies Involving Barriers

In these studies we assume that a contaminant plume occupies a 250 m (820 ft) square area in an aquifer with a natural regional flow of 0.3 m/day (1 ft/day). With the aquifer permeability assumed to be 20 darcies (2×10^{-11} m^2), this regional flow corresponds to a head gradient of approximately 0.02. The cases studied are listed in Table 1. In each case we study the areal (x, y) evolution of the plume. Case 1 is a reference case without any barriers. Figure 1 shows the time development of the plume from its initial position to its position after 6 months. Only half of the region is shown because of symmetry. Initially the plume is arbitrarily assumed to be rectangular with contaminant concentration ranging from 1000 ppm to 100

Table 1. List of Cases Involving Barriers

1.	Without barrier	Basic case for comparison
2.	300 m barrier	Short barrier upstream
3.	450 m barrier	Long barrier upstream
4.	450 m, 20 millidarcies barrier	Long barrier with higher permeability
5.	Two barriers	Short barriers upstream and downstream
6.	300 m barrier with fracture zone	Zone 10 m wide with 10 times permeability

Note: All cases were modeled for 24 months with a regional flow of .3 m/day (1 ft/day) and a head gradient of approximately 0.02. The initial conditions are a 250 m (820 ft) square zone of contaminant with concentrations ranging from 1000 ppm to 100 ppm.

Physical Properties

	Aquifer	Low permeability Barrier	High permeability Barrier	Fracture Zone
Permeability (m^2)	2×10^{-11}	2×10^{-19}	2×10^{-14}	2×10^{-10}
(darcies)	20	2×10^{-7}	2×10^{-2}	200
Porosity	0.10	0.01	0.01	0.10

All media have a constant compressibility of 2×10^{-10} Pa^{-1} and are isotropic. All fluid properties are for pure water at 20°C.

ppm. After 6 months, the plume has moved downstream with the regional flow. The spreading shown in the figure is due to numerical dispersion. In simple geometries such as this, numerical dispersion produces results which qualitatively resemble physical dispersion.

Studies were made (Cases 2-6) involving various kinds of barriers, as well as the presence of a fracture zone. The presence of a low-permeability

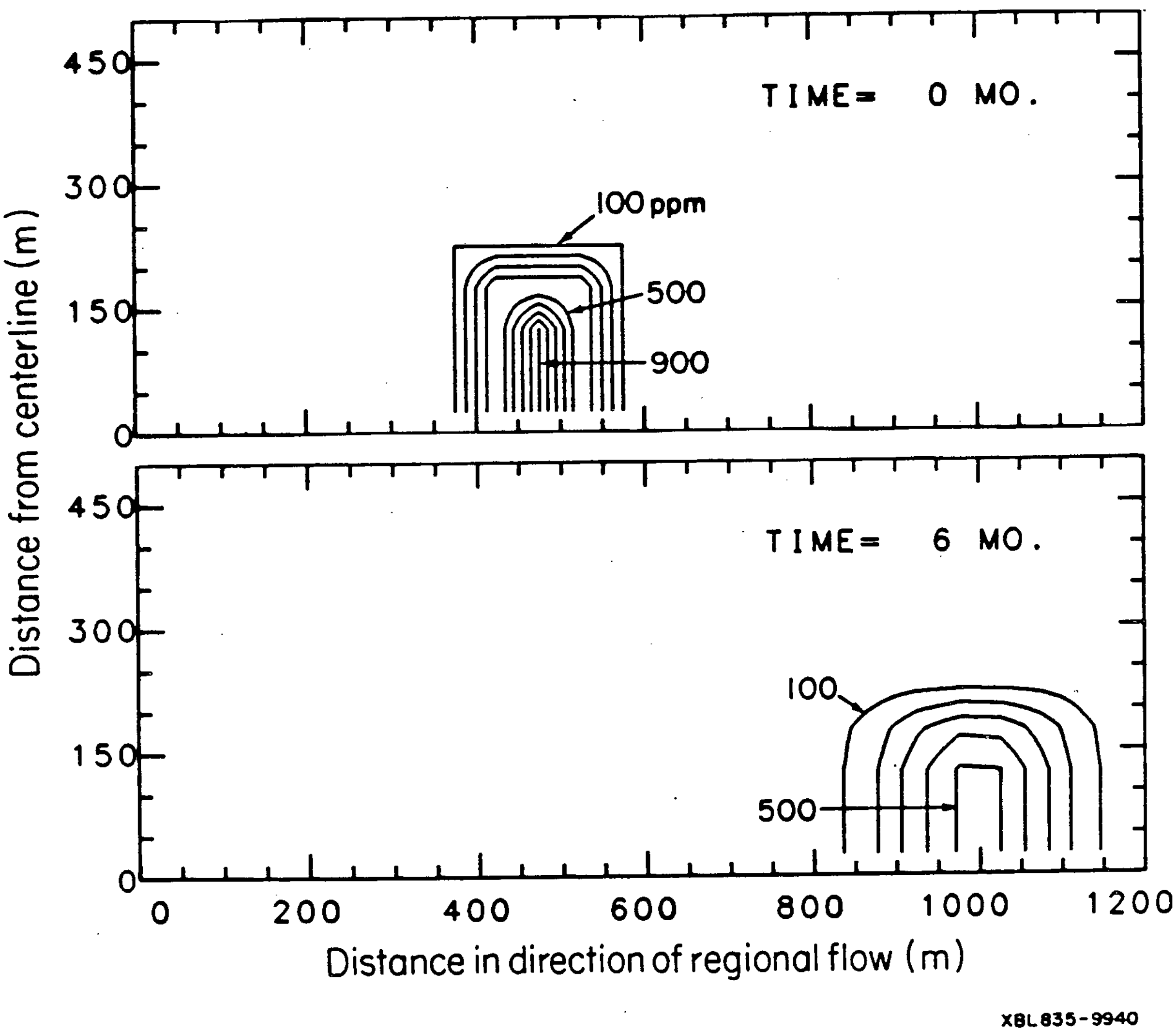

Figure 1. Regional flow with no barrier: Concentration contours (at increments of 100 ppm) for the plume in its initial condition and after 6 months.

barrier upstream of the plume slows down its movement (Case 2). As one would expect, this effect is enhanced for a longer barrier (Case 3). These cases are shown in Figures 2 and 3 respectively. Case 4 represents a case similar to Case 3, except that the barrier is assumed to be 10^5 times more permeable than that in Case 3. It is interesting to note that Case 3 and Case 4 give almost identical results (Figures 3 and 4). Thus once the barrier is less permeable than the aquifer by a certain factor (in this case 10^3), an even less permeable barrier will not improve the effectiveness of the plume control operation.

Case 5 shows the case of two barriers, one upstream and one downstream of the contaminant plume. As can be seen in Figure 5, the containment is quite impressive. The lowest contaminant density contour shown (100 ppm) is completely prevented from escaping. However contaminant still escapes, though at a much lower concentration level. Figure 6 shows the same data as Figure 5, with a smaller contour interval. The lowest two contour levels correspond to 25 and 50 ppm. An interesting dilution effect is apparent.

The presence of a fracture zone alters the situation drastically (Case 6). The fracture is represented by a zone of high permeability which has a much higher regional flow velocity. This high-flow channel becomes a fast path for the contaminant to leak downstream (Figure 7). Although the low-permeability barrier seals the fracture zone at one point, the regional flow goes around the barrier in the surrounding porous medium and then returns to the fracture zone to transport the plume away. The plume is displaced significantly in just 4 months.

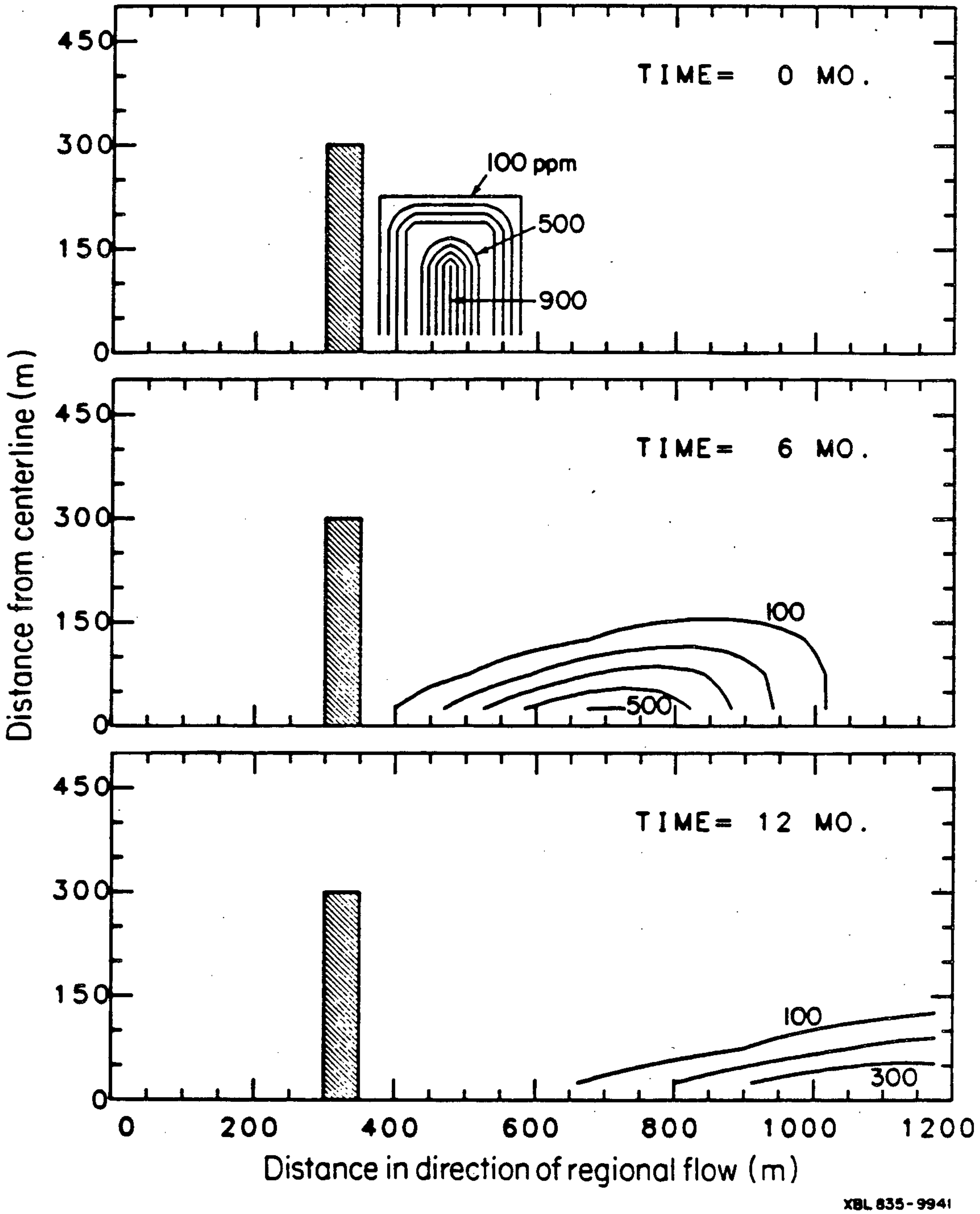

Figure 2. Regional flow with 300 m barrier: Concentration contours (at increments of 100 ppm) for the plume in its initial condition and after 6 and 12 months.

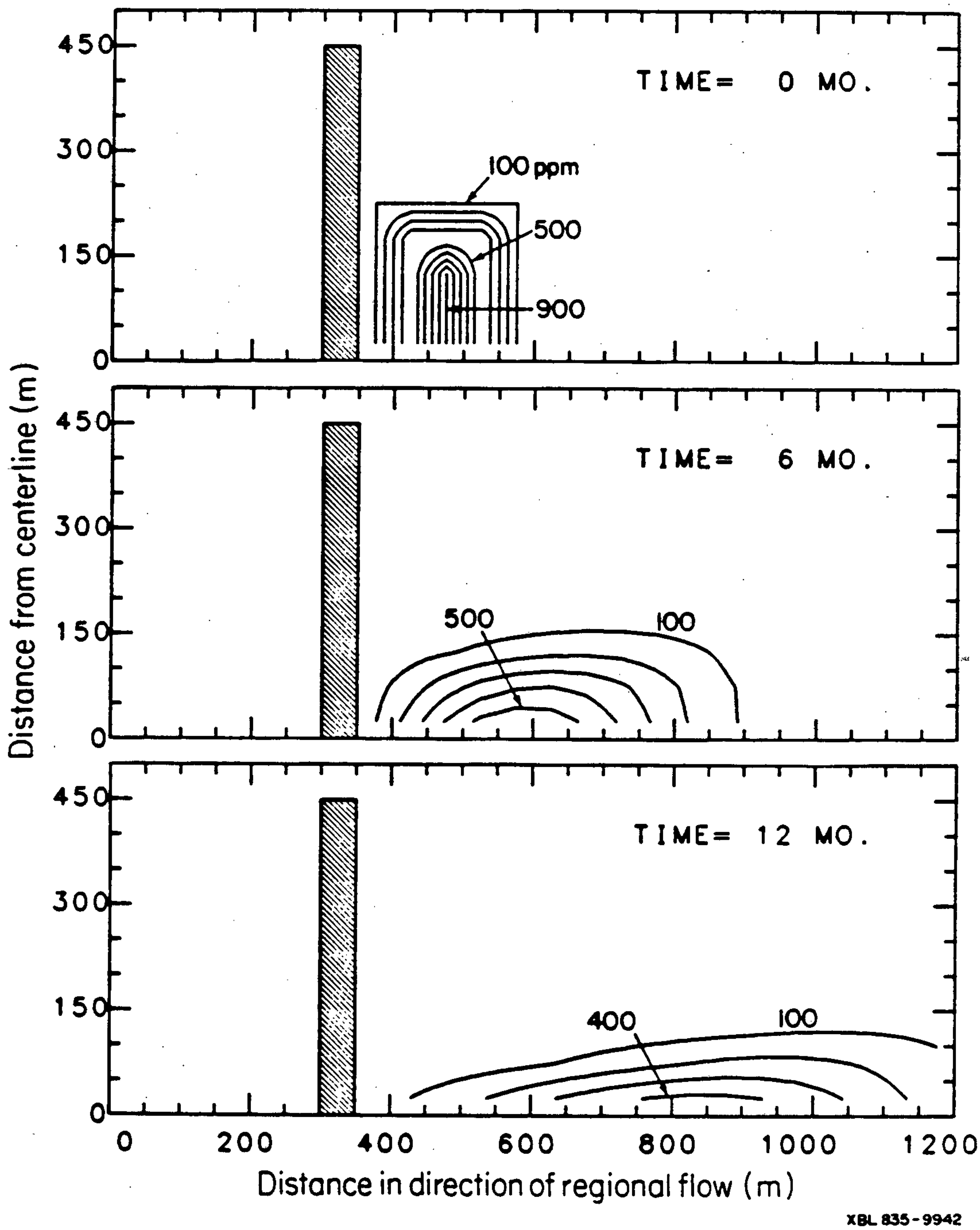

Figure 3. Regional flow with 450 m barrier: Concentration contours (at increments of 100 ppm) for the plume in its initial condition and after 6 and 12 months.

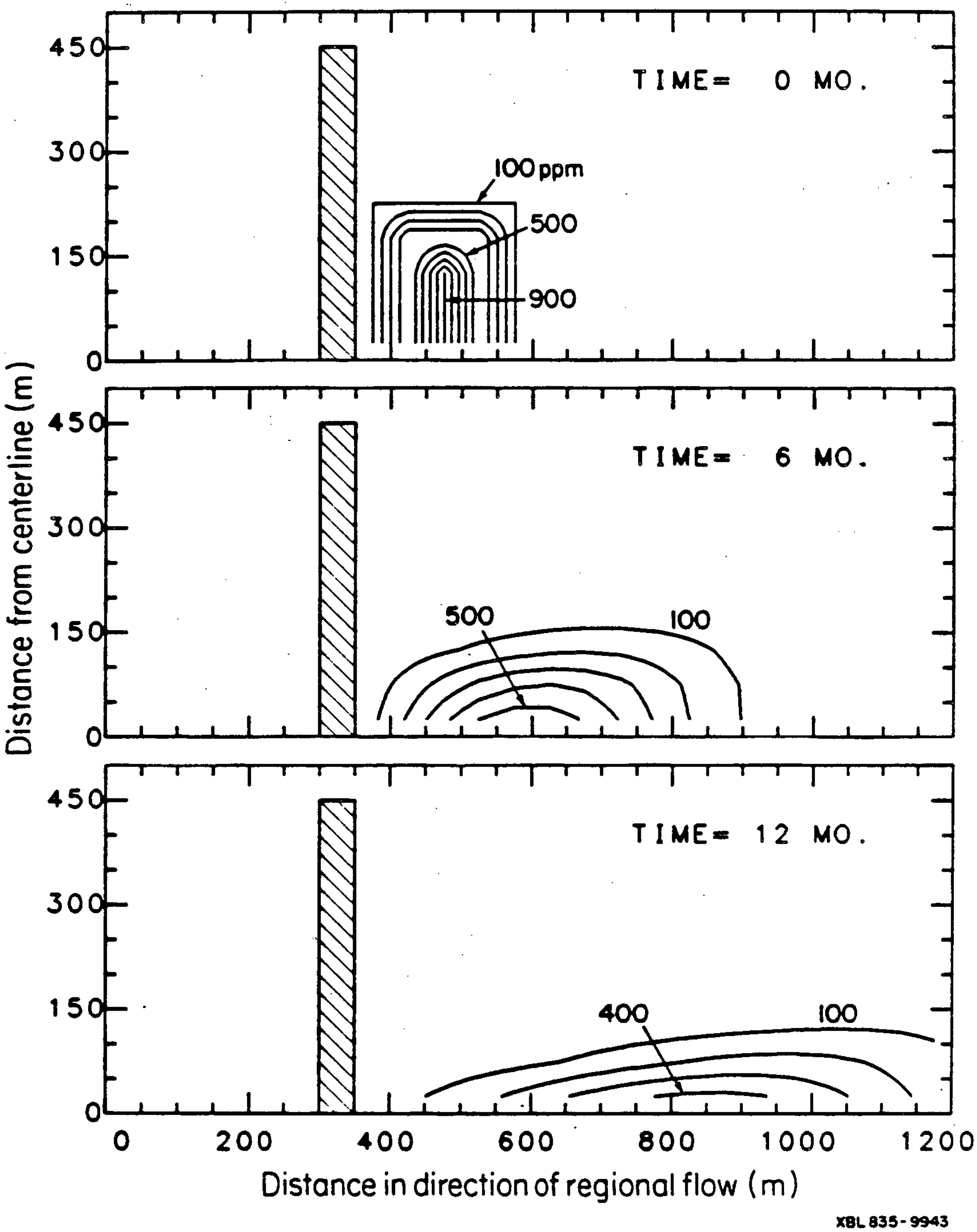

Figure 4. Regional flow with 450 m, 20 mD barrier: Concentration contours (at increments of 100 ppm) for the plume in its initial condition and after 6 and 12 months.

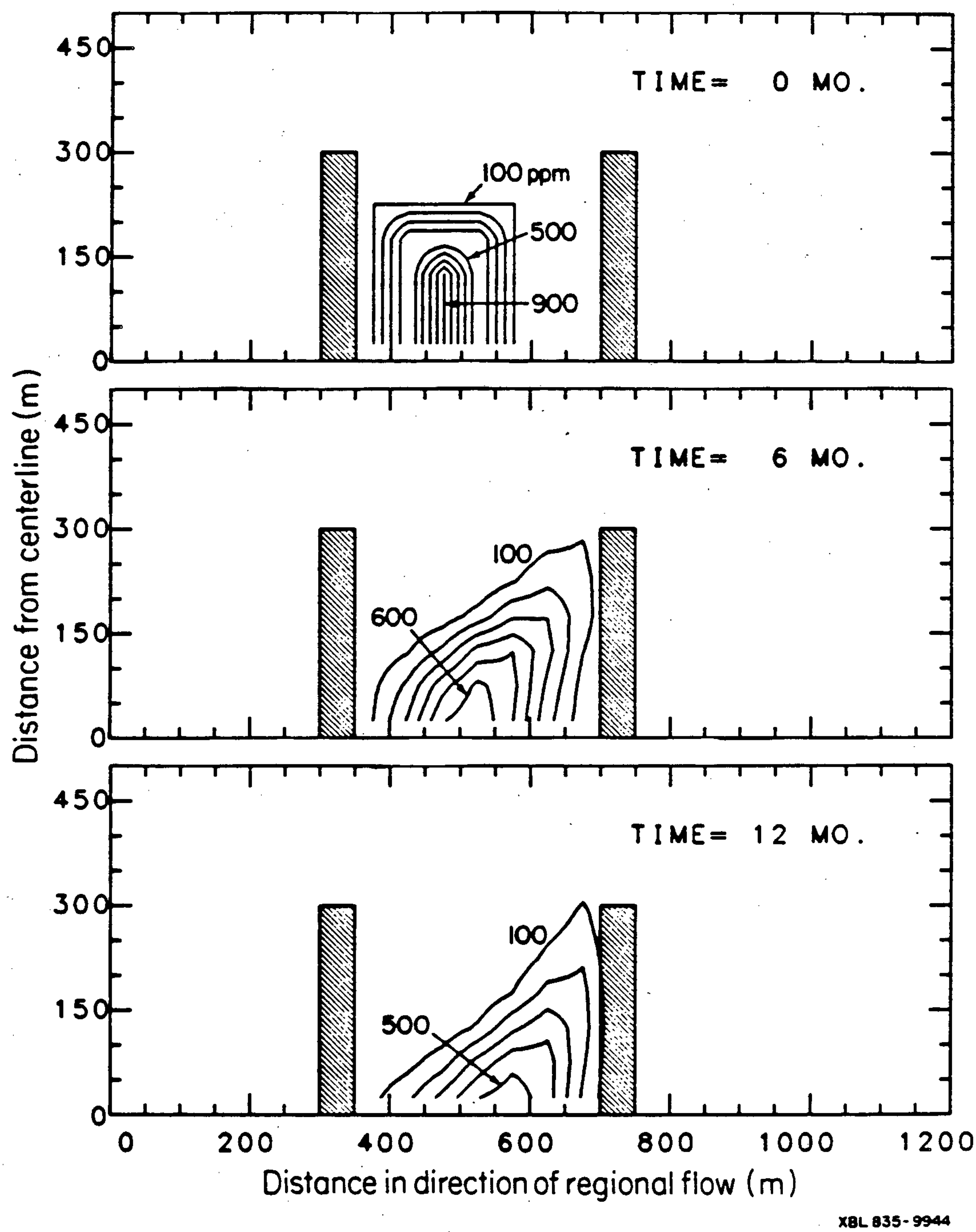

Figure 5. Regional flow with two 300 m barriers: Concentration contours (at increments of 100 ppm) for the plume in its initial condition and after 6 and 12 months.

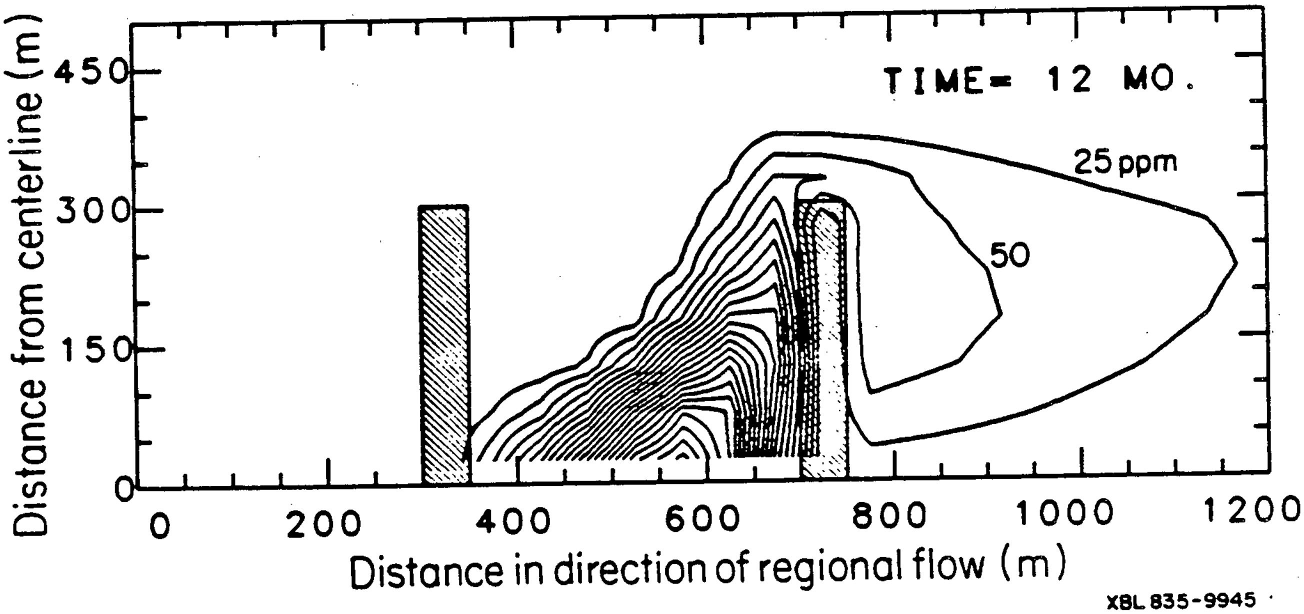

Figure 6. Regional flow with two 300 m barriers: Concentration contours (at increments of 25 ppm) for the plume after 12 months.

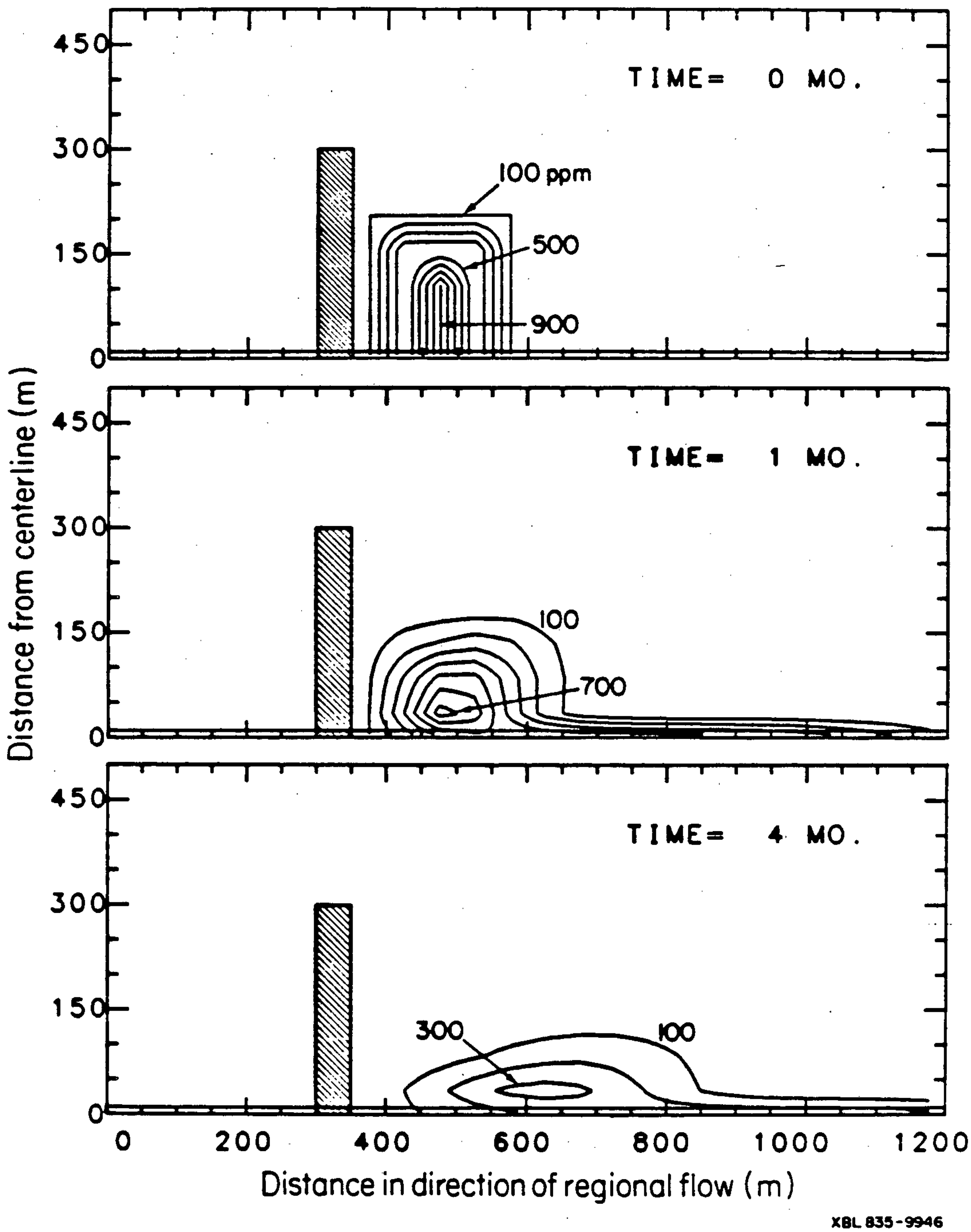

Figure 7. Regional flow with 300 m barrier and fracture zone: Concentration contours (at increments of 100 ppm) for the plume in its initial condition and after 1 and 4 months.

Comparative Studies Involving an Extraction Well

In these studies, we assume an axisymmetric system and study contaminant plume evolution in an (r, z) vertical section of a confined aquifer which is 21 m thick. The contaminant plume is formed due to infiltration into the top of the aquifer through a circular area 24 m in diameter centered at r = 0. Infiltration occurs for a period of one year. After infiltration stops, extraction through a well located at r = 0 begins. The parameters of the system are shown in Table 2.

Table 2. Physical Properties for Extraction Cases

Aquifer Thickness = 21 m
Closed boundaries above and below the aquifer (except for infiltration zone)
Hydrostatic pressure boundary at r = 16 km

Contaminant Plume Formation		
Infiltration rate	= 1.38 kg/sec	= 22 gpm
Infiltration period	= 1 year	
Infiltration zone, radius	= 0-12 m	
Aquifer Properties		
Permeability	= 2×10^{-11} m^2	= 20 darcies
Porosity	= 0.20	
Compressibility	= 1×10^{-8} Pa^{-1}	
Isotropic material		
Two-layered Aquifer Case		
Permeability of upper layer	= 2×10^{-11} m^2	= 20 darcies
Permeability of lower layer	= 4×10^{-11} m^2	= 40 darcies
Horizontal Fracture Case		
Fracture zone thickness	= 1 m	
Fracture zone permeability	= 2×10^{-10} m^2	= 200 darcies

A measure of the effectiveness of contaminant extraction is called the recovery factor, ε^*, which is the percentage of contaminant extracted when the volume of fluid extracted is equal to the total volume of infiltrated contaminated fluid. In the following, V_i is defined to be the fraction of infiltrated fluid over the total volume infiltrated during one year, and V_e to be the fraction of extracted fluid over the total volume of infiltrated fluid. Thus for $\varepsilon^* = 1$, the extraction operation is completely successful--all the contaminant that infiltrated into the aquifer is withdrawn (at $V_e = 1$) without any mixing with the aquifer water. If ε^* is much less than one, it indicates that there is much mixing between contaminated and aquifer water so that the clean-up action is not as effective. One then has to produce a large volume of water to extract a sufficient amount of the contaminant.

Different extraction cases studied are summarized in Table 3. Case A represents the case where extraction is from a well that penetrates the upper 38% of the aquifer. In Figure 8, the top graph shows the concentration contours after one year of contaminant infiltration, before extraction begins. After one year of extraction the recovery factor ε^* is 0.89; the contaminant remaining in the aquifer is shown in the bottom graph of Figure 8.

Cases B, C and D study the effect of a two-layered aquifer. The lower layer is assumed to be twice as permeable as the upper one. Figure 9 shows a time sequence of concentration contours during extraction for case D, where extraction is from the upper 38% of the aquifer. The top graph shows contaminant concentration just before extraction begins. The increased plume flow into the higher permeability lower layer is apparent. During extraction,

Table 3. Summary of Extraction Cases

	Extraction Well Screen Interval	ε^*
Homogeneous Aquifer		
Case A	Upper 38% of aquifer	0.89
Lower Half of Aquifer with Double Permeability		
Case B	Full Aquifer Thickness	0.87
Case C	Lower 33% of aquifer	0.85
Case D	Upper 38% of aquifer	0.89
Horizontal Fracture with 10 Times Aquifer Permeability		
Case E	Upper 38% of aquifer	0.85
Case F	At fracture, 10% of aquifer thickness	0.84
Heavy Contaminant in a Homogeneous Aquifer		
Case G	Full aquifer thickness	0.25
Case H	Lower 33% of aquifer	0.36
Case I	Lower 10% of aquifer	0.37

In each case rate is 1.38 kg/sec (22 gpm), ε^* is defined for one year of extraction.

fluid again moves faster in the lower part of the aquifer allowing the timely extraction of a large portion of the plume there. After one year of extraction, $V_e = 1$ and the recovery factor is 0.89. Figure 10 shows the contaminant remaining in the aquifer after one year of extraction for cases B, C and D, corresponding to extraction from the full aquifer thickness, from the lower (high permeability) part of the aquifer, and from the upper (low permeability) part of the aquifer respectively. The maximum contaminant concentration is lowest for case D; this result is contrary to the commonly held belief that extraction from high permeability zones of layered aquifers is best.

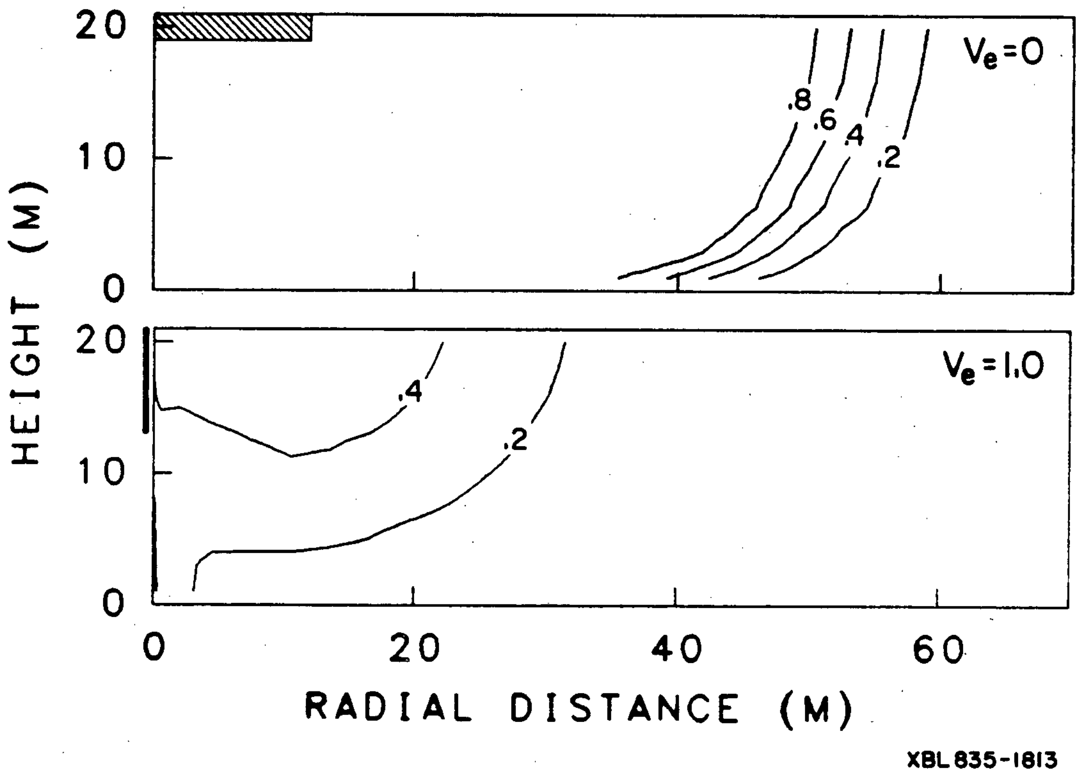

Figure 8. The upper graph shows calculated concentration contours after 1 year of contaminant infiltration through the shaded region, before extraction has begun ($V_e = 0$). The lower graph shows contours after plume extraction ($V_e = 1$) through the well marked by the vertical segment.

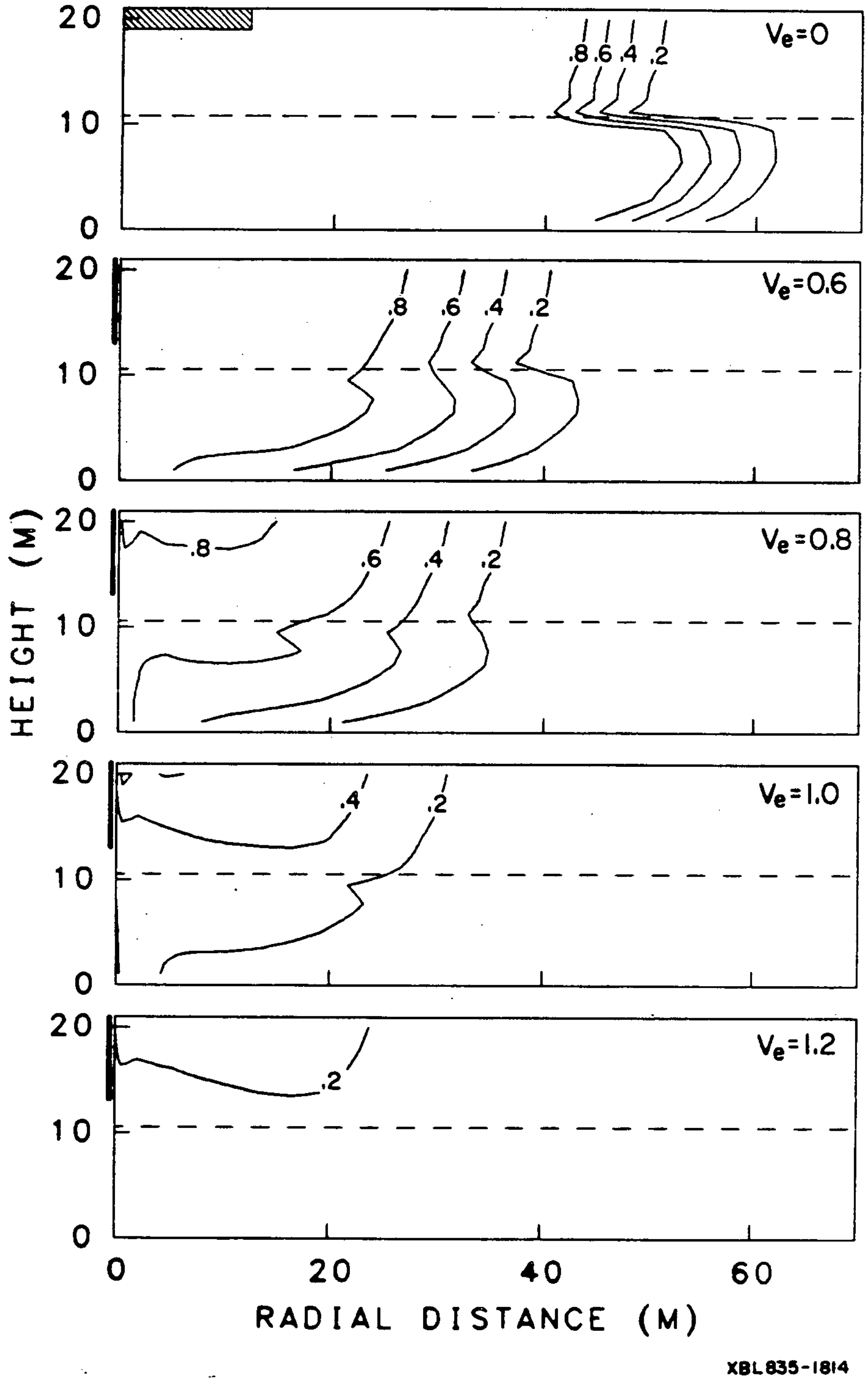

Figure 9. A time sequence showing the extraction of a contaminant plume from a two-layer aquifer. The permeability below the dashed line is double that above it. The infiltration zone is shaded; the extraction well is marked by the vertical segment.

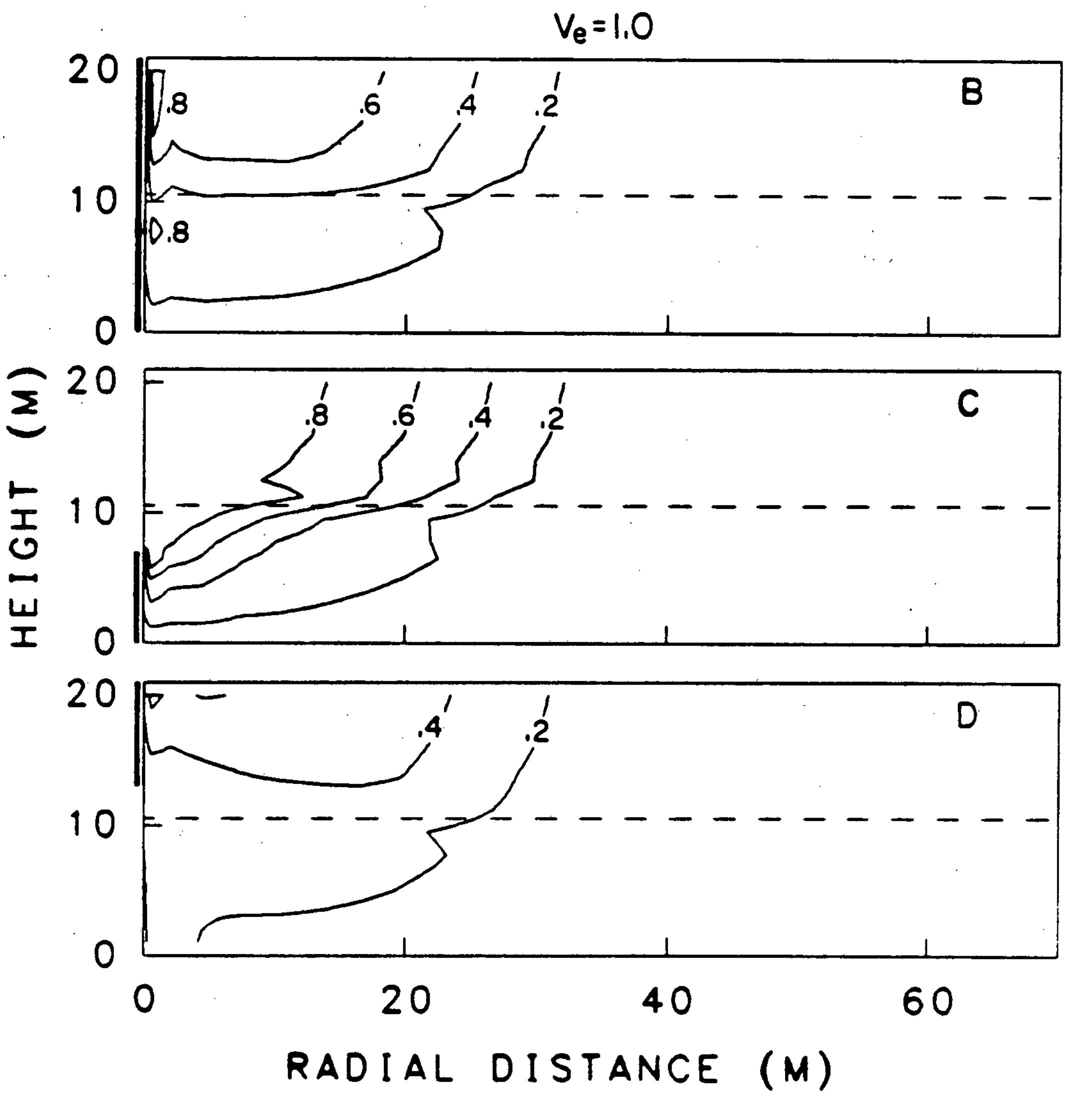

Figure 10. The concentration contours in a two-layer aquifer after plume extraction (V_e = 1) for three different extraction wells (Cases B, C, D). The original plume (V_e = 0) was as shown in the top graph of Figure 9. The vertical segments show each extraction well.

The effect of the presence of a high-permeability fracture zone is studied in cases E and F. The fracture zone acts as a fast path for the plume, as shown in Figure 11. The top graph in Figure 11 shows the calculated concentration contours just before extraction; the lower two graphs show the contaminant concentration after extraction from the upper part of the aquifer and from near the fracture zone level. The recovery factors for the two cases are about the same.

The final series of studies involves the extraction of a contaminant plume with density 4% higher than that of the groundwater. Even with such a slight density difference, the plume tends to flow to the bottom of the aquifer. Figure 12 shows the concentration contours as the contaminated fluid infiltrates into the aquifer. The extractions by different well penetration arrangements, cases G, H and I, all show a rather poor recovery factor (Table 3 and Figure 13). This implies that one has to be rather careful about this situation, because even though the contaminant concentration of the extracted water decreases to a low value, there may remain in the lower part of the aquifer a significant amount of contaminant plume which may not be detected by a monitoring system that samples only the upper part of the aquifer.

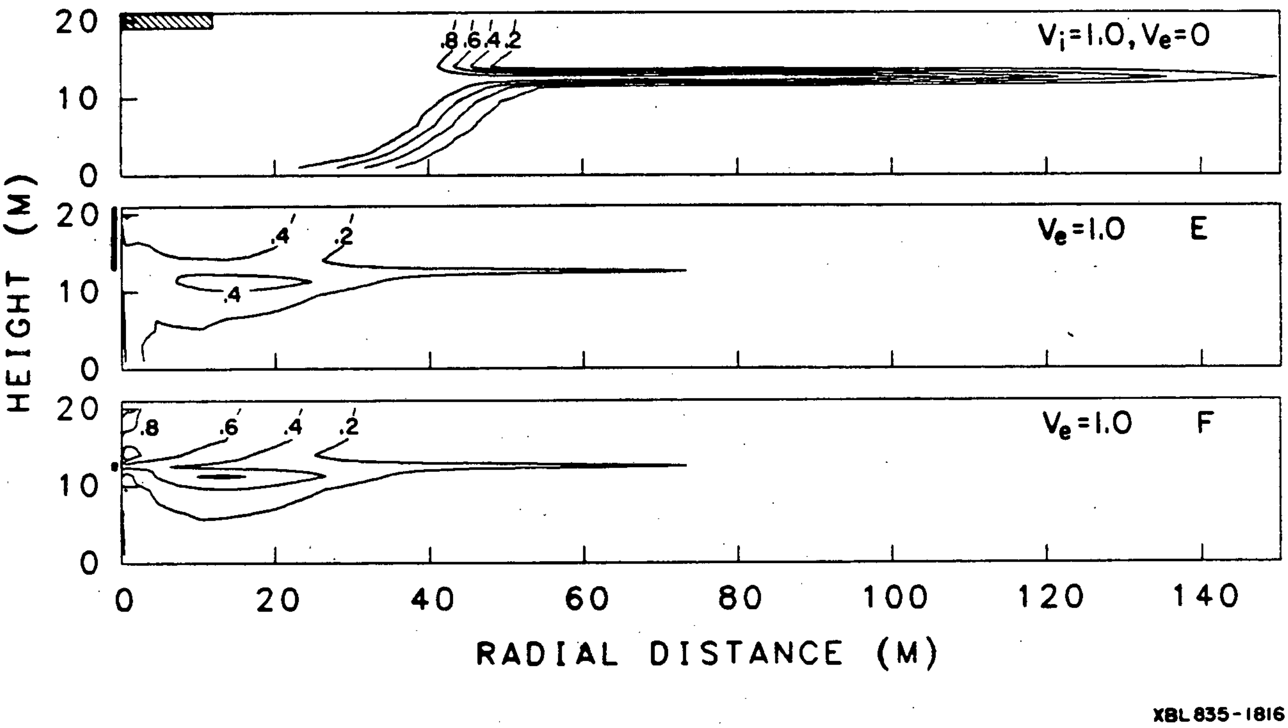

Figure 11. The top graph shows concentration contours after 1 year of contaminant infiltration into an aquifer with a horizontal fracture. The lower graphs show the contaminant contours after extraction (V_e = 1) for two different extraction wells (Cases E and F).

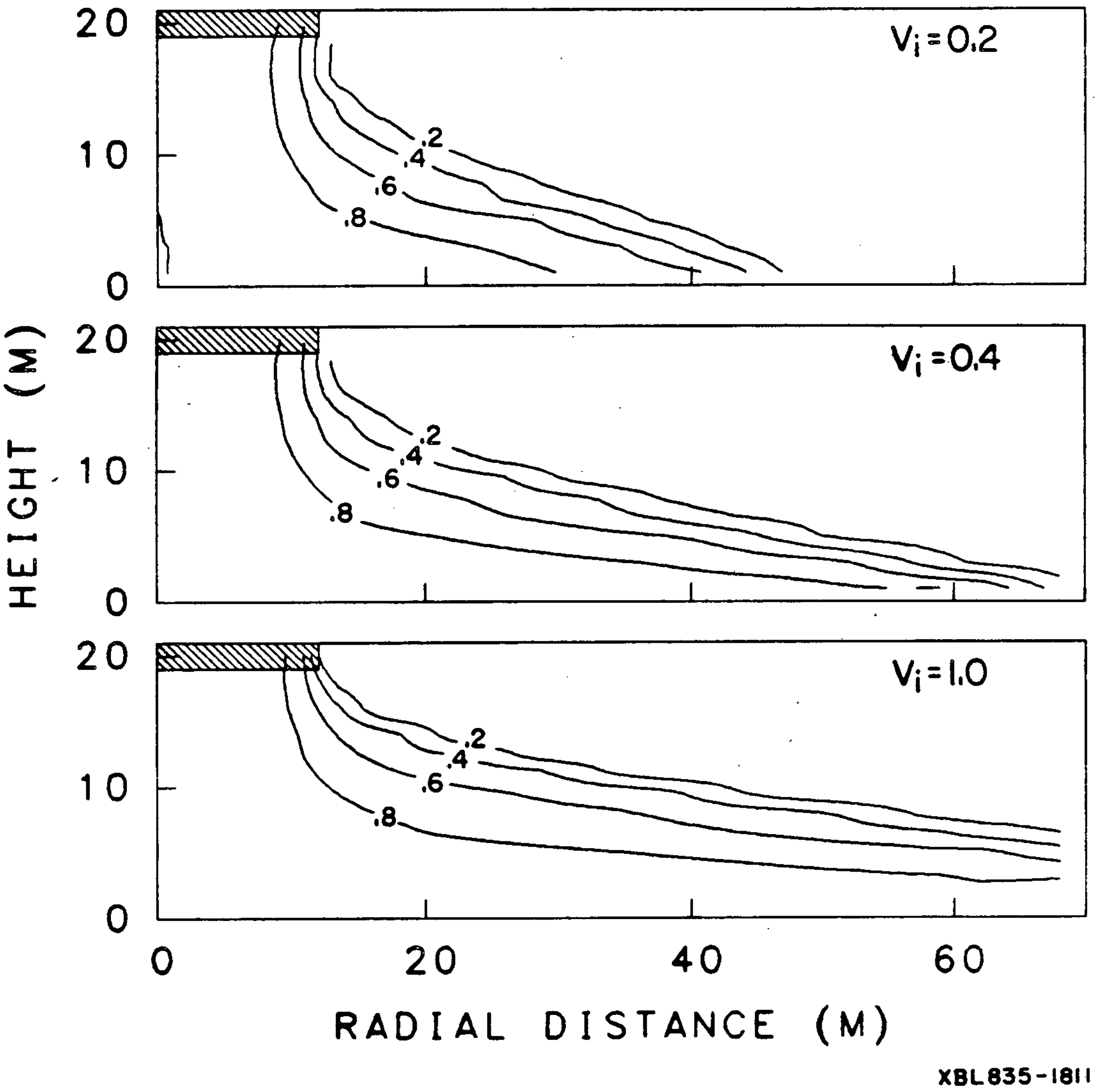

Figure 12. A time sequence showing the infiltration of a heavy contaminant plume into a homogeneous aquifer.

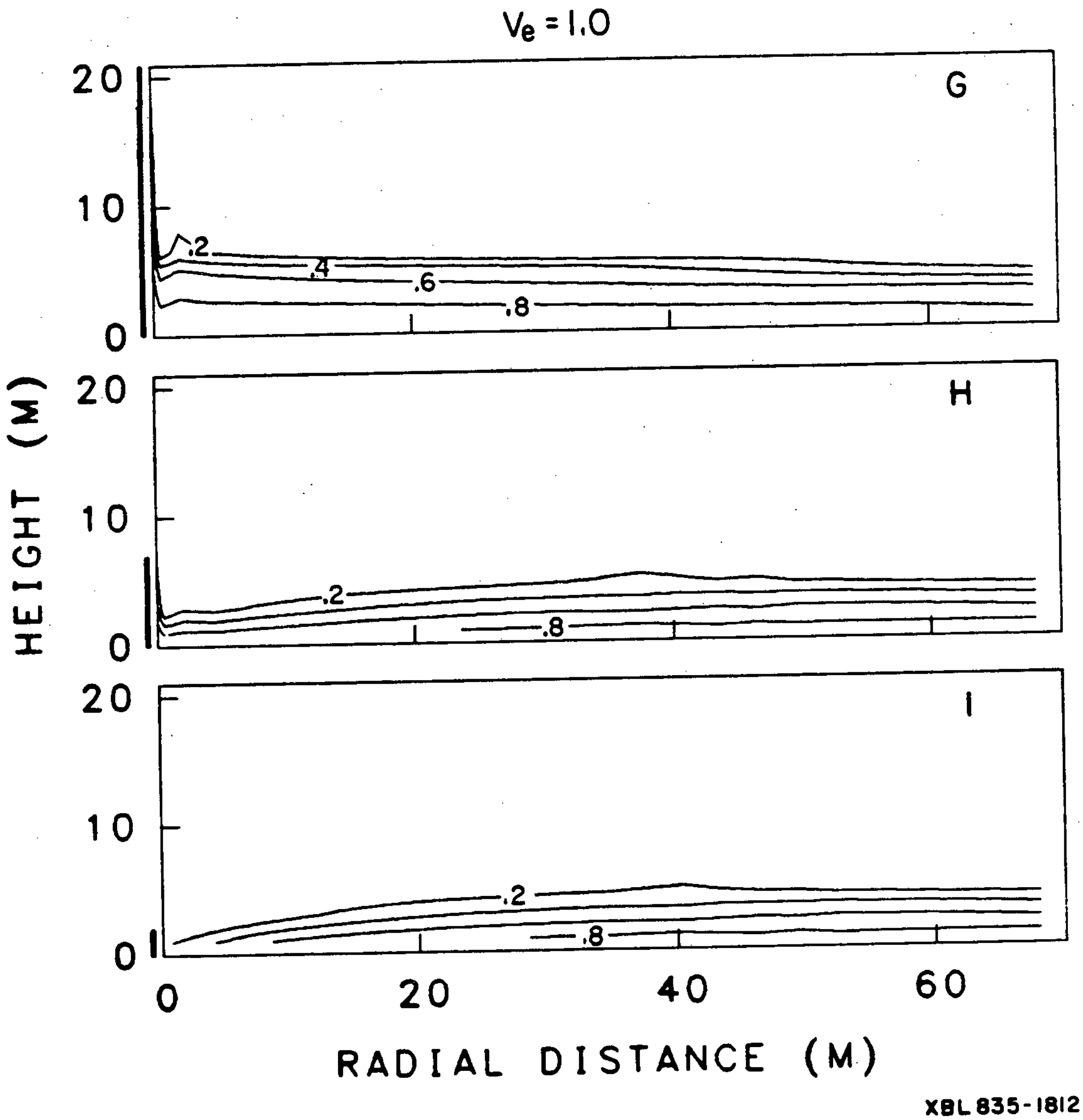

Figure 13. The concentration contours after extraction (V_e = 1) of a heavy plume through three different extraction wells (Cases G, H, I). The original plume (V_e = 0) was as shown in the bottom graph of Figure 12.

Conclusion

The present investigation has two goals. The first is to demonstrate the capability of mathematical modeling techniques to study contaminant plume control and extraction procedures. The second is to explore generically what is expected to happen for a series of contaminant plume control and extraction scenarios. Further work is underway to study the implications from the results of this work.

Acknowledgements

The present paper is based on work done under Interagency Agreement Number AD89F 2A 175 between the U. S. Environmental Protection Agency and the U. S. Department of Energy and under Contract DE-AC03-76SF00098.

References

[1] Mangold, D. C., and Tsang, C. F., 1983. Development of a three-dimensional transient thermohydrological parcel model with chemical transport and reactions. In preparation.

[2] Bodvarsson, G. S., 1982. Mathematical modeling of the behavior of geothermal systems under exploitation. Ph.D. Thesis, University of California, Berkeley (LBL-13937).

[3] Buscheck, T. A., Doughty, C., and Tsang, C. F., 1983. Prediction and analysis of a field experiment on a multilayered aquifer thermal energy storage system with strong buoyancy flow, Water Resources Research, in press.

[4] Tsang, C. F., Buscheck, T. A., Doughty, C., 1981. Aquifer thermal energy storage--A numerical simulation of Auburn University field experiments. Water Resources Research, 17(3), p. 647-658.

TECHNICAL INFORMATION DEPARTMENT
LAWRENCE BERKELEY LABORATORY
UNIVERSITY OF CALIFORNIA
BERKELEY, CALIFORNIA 94720